Theoretical and experimental investigation of the deformation shape in press-braking bending considering surface residual stresses induced by milling operation

Min Zhang (zm@xpu.edu.cn)
Xi'an Polytechnic University
Dongming Li

Research Article

Keywords: press-braking bending, milling-induced residual stress, final shape, springback, aluminum alloy sheets

Posted Date: May 17th, 2023

DOI: https://doi.org/10.21203/rs.3.rs-2904641/v1

Version of Record: A version of this preprint was published at The International Journal of Advanced Manufacturing Technology on February 1st, 2024. See the published version at https://doi.org/10.1007/s00170-024-13089-7.

Abstract

Press-braking bending is usually performed after face milling to obtain the specified curvature of variety mechanical parts, which is widely applied in the aircraft manufacturing. The surface layer residual stress on workpiece caused by milling has an important influence on subsequent forming. The influences of surface residual stress caused by milling operation on press-braking bending has been investigated analytically and experimentally in this study. The analytical model for springback prediction based on plane strain assumption is proposed using the material model of Mises yield criterion and Swift exponential hardening law, and takes into account of the effects of milling-induced residual stress. Three levels of residual stress are introduced in the test plates through milling operation with different cutting speed. The analytical results are compared with the bending experiments of 7050-T7451 Al-alloy plates. Results show that the accuracy of the contour obtained by the proposed model is improved when surface residual stress is considered. Furthermore, the influence of surface residual stress on springback is discussed. It is revealed that surface tensile residual stress increases springback and surface compressive residual stress contributes positively to the final shape of bent specimens.

1 Introduction

Press-braking bending is a metal forming process in which the universal dies are used to carry out local three-point bending point by point according to a certain deformation sequence, and then the ideal curvature shape can be obtained through successive accumulation of bending deformation [1]. These processes have many advantages, such as strong adaptability to different contours, simplicity of bending tools, short manufacturing time and low process cost [2, 3]. Due to these advantages, press-braking bending has been widely used in the manufacture of aircrafts [4], marine engineering structures, ship hull structures, and many other manufacturing fields [5, 6].

Press-braking forming process is an elastoplastic process, including loading and unloading. Springback will occur during unloading and directly influence the shape accuracy of formed plates. Therefore, it is of great importance to predict springback accurately. Different methods, such as analytical method, semi analytical method [7], finite element (FE) method and experimental method [8], have been applied to predict the springback of press-braking bending. YAN et al [9] improved the simulation accuracy of press bending by investigating the parameter identification method to determine the parameters of yield criterion. KIM et al [10] used FE analysis to estimate the stress and strain of a sheet being bent in pressbrake bending. ESAT et al [11] analyzed bending and springback of different aluminum materials of different thickness through FE analysis. However, FE method is a time-consuming method and is very sensitive to numerical parameters such as element type and size, contact definition and convergence criterion for solution. Analytical method is time saving but can only used to simple problems [12]. Only few studies have been reported for press-braking bending using analytical method. ANOKYE-SIRIBOR et al [13] developed an analytical model of the air bending process based on in-process identification of material characteristics during pressbrake forming. ZHAO [14] addressed a new analytical method for springback of small curvature plane bending with unloading rule of classical elastic-plastic theory.

MOHAMMADI et al [15] developed an analytical formulation for springback prediction based on a wrap around assumption and primary bending theories. The above analytical models have good agreement between the predict results and experimental data. However, on one hand, springback prediction is investigated in single-point bending forming in the above studies. Press-braking bending is a multi-step bending process at different bending points, and the final shape of bent plates need to be concerned. On the other hand, as the extra materials have been removed via face milling operation prior to bending submission, especially for large integral panels, a high level of surface residual stresses are generated [16] in the prepared plates. The milling-induced residual stresses have been studied extensively in terms of machining techniques [17–19], but have not been considered in springback for press-braking bending. WEISS et al [20] and ABVABI et al [21, 22] indicated that the product quality of sheet metal may be affected by the pre-existing residual stress during bending forming. LIN et al [23] demonstrated that both residual stress and thickness have major effect on sheet metal's springback. However, the existing springback theory and finite element simulation rarely consider the impact of milling-induced surface residual stress, which may lead to a certain error with regard to the springback prediction and contour accuracy of bent plates. This has raised the idea of studying press-braking bending combining with surface residual stress.

A few studies have been performed on the influences of pre-existing residual stresses on the forming of sheet metal. A commercial aluminium alloy, AA6063, was reduced in thickness by rolling to introduce residual stresses into the material, and finite element analysis was used to analyze the effect of residual stresses on downstream forming. The results show that including the effect of pre-existing residual stresses will improve model accuracy [20, 22]. An experimental study of surface residual stress for deformation machining (a combination of thin structure machining and single point incremental forming/bending) has been performed by SINGH [24], and the effect of machining parameters, bending parameters and forming parameters on surface residual stress were discussed. However, the effect of surface residual stress induced by machining on subsequent forming/bending is not considered. HUANG et al [25] introduced machining-induced residual stresses on the surface of the components to investigate the effect of residual stress on machining deformation for monolithic component. WANG [26] studied the influences of initial residual stress of blanks and cutting stress in the machining process on deformation of thin-walled parts, and the results showed that initial residual stress and cutting stress have a significant effect on workpiece deformation after processing. In their work, the influences of residual stress on machining deformation for monolithic component are analyzed based on finite element simulations and experiments, and the results show that the initial stresses influence the subsequent process to some degree. A creep model is developed by SPENCE [27] to describe the effect of residual stress due to machining operations on the geometry of an aluminum alloy component as it creeps. Finite element models have been developed to simulate creep-age forming (CAF) processes with consideration of machining-induced residual stresses and distortion by LAM [28], and the results showed that the machining-induced residual stresses will affect the accuracy of springback prediction in CAF. The theoretical model and numerical method are proposed by LI [29] to investigate the machining distortion of the pre-bent cylindrical skin-panels. The residual stresses due to the coiling-uncoiling process are

specified as the initial stresses in a subsequent finite element simulation of cold bending by QUACH [30, 31]. LI et al [32] investigated the effect of machining-induced stresses on springback of creep age formed AA2050 plates experimentally and numerically, and different levels of residual stress were assigned to the test plates with different thickness. Overall, the influences of surface residual stress on press-braking bending have not been investigated, and the final shape of bent plates need to be concerned for multi-step bending.

In this study, the influences of surface residual stress caused by milling operation on the press-braking bending is investigated through analytical modeling and experiments. The analytical model for springback prediction based on plane strain assumption are proposed using the material model complying with Mises yield criterion and Swift exponential hardening law, and takes into account of the effects of milling-induced residual stress. Three levels of residual stress are introduced in the test plates through milling operation with different cutting speed. The analytical results are compared with the bending experiments of 7050-T7451 Al-alloy plates. Further analyses of the effect of surface residual stress on springback and final shape of the plates have been carried out and conclusions are given at the end of the paper.

2 Milling-induced surface residual stresses

Milling is widely used for manufacturing various parts, which will cause severe mechanical and thermal stress on the material and then result in the formation of residual stress on surface layer of the machined parts [33]. The experimental method [34], FE method [35] and analytical model [19] are used to study the influence of the cutting parameters, tool geometry, cutting edge geometry, tool wear, and cutting tool material on the residual stresses. In this study, surface residual stresses are introduced into the sheets using three different cutting speed conditions for the cutting speed has a significant influence on residual stress.

The residual stresses at the surface of the workpiece show a certain degree of dispersion, and this is mainly due to the different cutting forces and cutting heat at different geometric position on workpiece. However, compared with the effect of cutting speed on residual stress, the change of geometric position has little effect on residual stress. Additional, the residual stress are distributed in plane stress condition [36], and the stress perpendicular to the feeding direction, which is parallel to the bending direction, has little effect on bending deformation. Therefore, the stresses discussed in this research are the surface residual stress in feeding direction of milling.

3 Analytical springback model considering surface residual stresses

When the sheet is bent, the stress distribution in the cross section with consideration of the initial stress is shown in Fig. 1. In this paper, the residual stress is taken into consideration in the theoretical analysis of the workpiece bending. The cross section can be divided into three regions, i.e., the superposition areas in

upper and lower surfaces and remaining area. Therefore, the stress distribution in the superposition areas inherits the bending stress and the milling-induced stress.

The following assumptions are listed to build the springback prediction model for sheet bending:

1. The volume of the material is constant during the bending process, which can be written as $\varepsilon_\theta + \varepsilon_b + \varepsilon_r = 0$, where ε_θ, ε_b, ε_r represent the strain components in the direction of tangential, radial, and thickness.
2. The plane strain condition, ε_b= 0, is adopted during press-braking bending for wide plate.
3. The contact region between punch and sheet is assumed to be circular [37], and the neutral surface always stay at the same position.
4. The material exhibits Swift exponent-hardening behavior, which satisfy the stress-strain law: $\overline{\sigma}=K\left(\varepsilon_0+\overline{\varepsilon}\right)^n$[38, 39], where ε_0 is material parameters given by $\sigma_0=K{\varepsilon_0}^n$, is strength coefficient, andis hardening exponent.
5. The shear stress is ignored during bending, and the arbitrary cross-section remains plane and perpendicular to the deformed middle surface of the sheet [40].
6. Von Mises criterion, which is suitable for the ductile materials, is used for plastic yielding,.

Due to the milling operation, the surface material inherits the bending stress and the milling-induced stress. The stress on the bent plate cross-section with consideration of surface residual stresses can be expressed as follows:

$$\sigma_\theta{}' = \sigma_\theta + \sigma_{mill}, \quad \rho_i \leqslant \rho \leqslant \rho_o$$

1

where σ_θ is the tangential stress during bending process without consideration of the milling-induced stress and distributes in the range of $[-t/2, t/2]$, which have been derived in our former study [41]:

For the elastic deformation zone

$$\sigma_\theta = \frac{E}{1\text{-}\nu^2}\ln\frac{\rho}{\rho_n} + \frac{\nu E}{(1-\nu^2)(1-2\nu)}\frac{y_e}{\rho_n} - \frac{\nu}{1-2\nu}\frac{2}{\sqrt{3}}K\left(\varepsilon_0 + \frac{2}{\sqrt{3}}\ln\frac{\rho_n + y_e}{\rho_n}\right)^n \quad (\rho_n - y_e < \rho < \rho_n + y_e)$$

2

and

$$\sigma_\theta = \begin{cases} \sigma_r - \dfrac{2}{\sqrt{3}}K\left(\varepsilon_0 - \dfrac{2}{\sqrt{3}}\varepsilon_\theta\right)^n & \rho_\mathrm{i} \leqslant \rho \leqslant \rho_\mathrm{n} - y_\mathrm{e} \\ \sigma_r + \dfrac{2}{\sqrt{3}}K\left(\varepsilon_0 + \dfrac{2}{\sqrt{3}}\varepsilon_\theta\right)^n & \rho_\mathrm{n} + y_\mathrm{e} \leqslant \rho \leqslant \rho_\mathrm{o} \end{cases}$$

3

where E is Young's modulus, and v refers to the Poisson ratio. ρ is the curvature radius of the measured point. ρ_n is the curvature radii of the neutral layer before unloading. y_e is half the thickness of elastic deformation. σ_r is stress in the radial direction. K is strength coefficient. n is hardening exponent. ε_0 is material parameter. ε_θ is the strain component in the tangential direction. ρ_i and ρ_o are the curvature radii of the innermost and outermost surfaces of the bent plate, respectively.

The milling-induced stress σ_{mill} can be expressed as below,

$$\sigma_{mill} = \begin{cases} \sigma_{res}^{surf}, & -t/2 \leqslant t \leqslant -t/2 + t_r, t/2 - t_r \leqslant t \leqslant t/2 \\ 0, & -t/2 + t_r \leqslant \rho \leqslant t/2 - t_r \end{cases}$$

4

where t_r is the thickness of surface stress in Fig. 2, σ_{res}^{surf} is the surface residual stress induced by milling operation.

The total cross-section stress is the superposition of bending stress and initial stress. The bending moment is defined below,

$$M = \omega \int_{\rho_i}^{\rho_o} \sigma_\theta{}' \left(\rho - \rho_n\right) d\rho$$

5

where ω is width of the cross section.

The elastoplastic curvature change is equal to the elastic curvature change caused by the bending moment based on the classical springback theory, i.e., the springback bending moment and bending moment are equal in quantity and opposite in direction. The curvature change after the springback is achieved below [42, 43],

$$\Delta K = \frac{1}{\rho_0} - \frac{1}{\rho_1} = \frac{M}{EI}$$

6

with $I = \omega t^3 / 12$, where is the moment of inertia of the cross section, ΔK is the springback curvature, ρ_0 and ρ_1 are bending radius of the neutral layer before and after unloading.

According to the length of neutral layer remains the same, $\rho_1 \alpha_1 = \rho_0 \alpha_0$, and with Eq. (18), the springback angle for the bent workpiece is obtained by:

$$\Delta\alpha = \alpha_0\text{-}\alpha_1 = \alpha_0 \left(1\text{-}\rho_0/\rho_1\right) \quad (7)$$

where $\Delta\alpha$ is springback angle, α_0 and α_1 are bending angle before and after unloading.

The detailed procedure used to solve for the springback curvature and springback angle is presented in Fig. 2. The effects of both the milling-induced stress and bending stress are considered in the SPM-RS model (springback prediction model with milling-induced stress). The milling-induced stress is not contained in the SPM-NRS model (springback prediction model without milling-induced stress) when the step 4 is ignored in the calculation flowchart.

4 Experiments

4.1 Uniaxial tensile tests

The material used in this study is an aluminum alloy 7050-T7451, whose main chemical composition is presented in Table 1.

Table 1
Main chemical composition of 7050-T7451 (wt.%)

Si	Fe	Cu	Mn	Mg	Cr	Zn	Zr
≤ 0.12	0.013	2.0-2.6	≤ 0.10	1.9–2.6	≤ 0.04	5.7–6.7	0.08–0.15

The basic properties of the material are obtained through a series of uniaxial tensile tests which were carried out in a universal testing machine CSS-44100 according to the standards GB/T228-2002. The tensile specimens are designed as shown in Fig. 3(a). The tensile process is given in Fig. 3(b). A total of three tests were performed and the average stress-strain curve is plotted in Fig. 3(c). The mechanical properties of the material are presented in Table 2.

Table 2
Mechanical properties for Al 7050-T7451

Density (g/cm^3)	Tensile strength (MPa)	Yield stress (MPa)	Elasticity modulus *E* (MPa)	Poisson's ratio v
2.73	502	442	66000	0.33

4.2 Measurement of surface residual stress

The milling experiment is performed on JDHGT400_A10H NC. The cutting tool used is 8 mm diameter solid carbide with three blade structure. The feed rate (1.5m/min) is kept constant for tests, and changing spindle speed (10000 r/min, 12000 r/min and 14000r/min) are set for specimens to introduce different

surface residual stresses. Figure 4(a) shows the milling process. The directionis parallel to the feeding direction and the directionis perpendicular to the feeding direction. The workpiece used in this work is a rectangular block with the dimension of 200mm*15mm*7.5mm (Fig. 4(b)).

The milling-induced residual stresses on the surface of the workpieces are measured using the LXRD MG2000 stress analyzer (Fig. 4(c)), and the results are shown in Table 3.

Table 3
Surface residual stress in the feeding direction

Feed rate (m/min)	**1.5**		
Spindle speed (r/min)	10000	12000	14000
Surface residual stress (MPa)	25.62	-20.57	-31.59

4.3 Bending forming tests

The bending experiment is performed on the CSS-44100 Electric Universal Testing Machine. The distance between the support bodies is 50mm. The punch displacements adopted in bending experiments are 3mm and 3.5mm. The diameters of punch and support bodies are 10mm and 30mm respectively. Figure 5 shows the bending experiment tools and specimen. The contours of the specimens after unloading are obtained by Creaform 3D scanner, which is displayed in Fig. 6.

5 Results and discussion

When the measured surface residual stress is considered, the curvature radius and bending angle of all the three specimens (No.1-No.3) after unloading are calculated using numerical integration method with Eqs. (17)-(19), and the analytical results are shown in Table 4.

Table 4
Theoretical values

No.	With milling-induced stress		
	Punch displacement (mm)	Curvature radius (mm)	Bending angle (º)
1	3.5	133.1385	21.7974
	3	165.7571	17.4485
2	3.5	132.4991	21.9026
	3	164.6092	17.5702
3	3.5	132.3475	21.9277
	3	164.3377	17.5992
No.	Without milling-induced stress		
	Punch displacement (mm)	Curvature radius (mm)	Bending angle (º)
1–3	3.5	132.7831	21.8558
	3	165.1184	17.5160

5.1 Effect of surface residual stress on final shape

The contours of the specimens after press-braking bending through experiment and theoretical calculation with the SPM-RS model and SPM-NRS model are illustrated in Fig. 7(a)-(c), and half of the specimen is plotted for its symmetries. The profile predicted with the theoretical calculation has a good consistence with the measurement, and the errors between the experiment and the SPM-RS model of the No.1–3 specimens are less than 10%. The possible reasons accounting for some deviations between theoretical calculation and experimental results may be attributed to the following reasons: (1) Only the initial surface residual stress in the feeding direction is taken into account, and the shear stress is ignored, which lead to the under estimation of surface stress. (2) The theoretical models are calculated under the assumption that the neutral surface does not move during the press-braking bending and springback. (3) The errors in experimental data can be attributed to various origins such as flaws in blank preparations, deviations in milling, bending operations, method of measurements and so on. However, the prediction accuracy can meet the engineering requirements from the engineering view of point [44].

Compared with the experimental results, the difference between the contours calculated with SPM-RS model and SPM-NRS model is small for the surface residual stress considered in SPM-RS model after milling operation is relatively low. However, the relatively small differences still can be seen and the comparison of maximum contour error of three test plates is shown in Fig. 7(d). The accuracy of the contour obtained with SPM-RS model is higher than the predictions made under the SPM-NRS model, and the maximum deflection of contour prediction has improved by 42.1% (from 3.39–5.85%), 6.4% (from

5.88–6.28%) and 14.6% (from 6.07–7.11%), respectively. It is in agreement with the results for the rolling forming presented previously by ABVABI [22, 45]. This discrepancies between the SPM-RS model and SPM-NRS model may be partly due to additional surface residual stress after milling which are accounted for in the SPM-RS model and the springback model gives lower moment values according to Eq. (17), but not in the SPM-NRS model.

The bow height of the three specimens are calculated as shown in Fig. 8. The bow height represents the vertical distance from the lowest point to the highest point of the outer profile of the bent specimen. It can be found that the bow height values predicted with SPM-RS model and SPM-NRS model are close for the slight surface residual stress introduced in theoretical models. Nevertheless, the bow heights predicted with SPM-RS are smaller than that predicted with SPM-NRS model. Some possible explanations for this are given blow: the milling operation introduces plastic deformation in the material surface and leads to a higher yield stress in the surface material of specimens due to strain hardening. Therefore, the loading force in bending will increase to make the surface material of specimens yield, which lead to the increase of springback after unloading and decrease the bow height of the specimens for the theoretical calculations.

In addition, the maximum error of bow height between experiment and SPM-RS is 10.2%, which can further verify the accuracy of the analytical model. Therefore, the analytical springback model considering surface residual stress proposed in this paper is sufficiently accurate to predict the deformation of milling plates during bending process.

5.2 Effect of surface residual stress on springback

To study the effect of surface residual stress on springback, the comparison of springback angle under punch displacement of 3mm and 3.5mm are shown in Fig. 9(a), (b). It is obviously that the springback angle increases with increasing punch displacement, and the trend has also been observed in previous study by PARSA [15, 46]. In addition, the springback angle of No.1 is larger than the value calculated with SPM-NRS when the tensile surface residual stress is considered in SPM-RS model, and the springback angle of No.2 and No.3 is smaller than the value calculated with the SPM-NRS model when the compressive surface residual stress is considered in SPM-RS model.

This can be explained by the yield deformation of the surface material subjected to tensile residual stress is later than that the surface material subjected to the compressive residual stress, and a higher loading force is needed for forming the specimen that surface material subjected to tensile residual stress. Take punch stroke of 3mm as an example, the force-displacement curves of the three specimens (Nos. 1–3) during loading are shown in Fig. 10. It is further confirmed that the loading force is higher when the surface material subjected to tensile residual stress than that the surface material subjected to the compressive residual stress.

According to the results, the surface compressive residual stress contributes positively to the final shape of bent specimens. It is consistent with the conclusions of SHEN [44] that the springback control in the

edge regions is the key to control the processing quality.

6 Conclusions

The influences of surface residual stress caused by milling operation on press-braking bending are investigated in this study. An analytical springback model with surface residual stress is established based on plane strain assumption and bending experiments have been carried out for verification. The following conclusions can be drawn:

1) The contour errors between the results obtained from the SPM-RS and those obtained from experiments are less than 10%, and the maximum error of bow height is 10.2%. The prediction accuracy can meet the engineering requirements from the engineering view of point.

2) The accuracy of the three test plates' contours obtained with SPM-RS is higher than that of the SPM-NRS, and the maximum deflection of contour prediction has improved by 42.1% (from 3.39–5.85%), 6.4% (from 5.88–6.28%) and 14.6% (from 6.07–7.11%), respectively.

3) The springback angle increases when the tensile surface residual stress is introduced in the test plates. The surface compressive residual stress in feeding direction of milling contributes positively to the final shape of bent specimens. It is very helpful for improving the accuracy of press-braking bending in actual industrial fabrication.

Declarations

Funding This work is funded by the Natural Science Basic Research Project of Shaanxi Province, China (grant number 2022JQ-526), the Key Laboratory of Road Construction Technology and Equipment of MOE, Chang'an University (grant number 300102252508), and the Doctoral Foundation Project of Xi'an Polytechnic University (grant number BS202121).

Competing interests The authors declare no competing interests.

Author contributions All authors contributed to the study conception and design. Material preparation, data collection, and analysis were performed by Min Zhang and Dongming Li. The first draft of the manuscript was written by Min Zhang, and all authors commented on previous versions of the manuscript. All authors read and approved the final manuscript.

References

1. Yan Y, Wan M, Wang HB, Huang L (2010) Optimization of press bend forming path of aircraft integral panel. T Nonferr Metal Soc 20(2): 294-301
2. Kuroda K, Kawakami T, Okui T, Akiyama M, Kiuchi M (2015) Influential factor to dimensional precision of cold-drawn tubes. P I Mech Eng B-J Eng 229(1): 100-109

3. Panthi SK, Ramakrishnan N, Ahmed M, Singh SS, Goel MD (2010) Finite Element Analysis of sheet metal bending process to predict the springback. Mater Design 31(2): 657-662
4. Munroe J, Wilkins K, Gruber M (2000) Integral Airframe Structures (IAS)—Validated Feasibility Study of Integrally Stiffened Metallic Fuselage Panels for Reducing Manufacturing Costs. Seattle, Washington: Boeing Commercial Airplane Group
5. Miranda SS, Barbosa MR, Santos AD, et al (2018) Forming and springback prediction in press brake air bending combining finite element analysis and neural networks. J Strain Anal Eng 53(8): 584–601
6. Froitzheim P, Stoltmann M, Fuchs N, et al (2020) Prediction of metal sheet forming based on a geometrical model approach. Int J Mater Form 13(5): 829–839
7. Panthi SK, Ramakrishnan N (2011) Semi analytical modeling of springback in arc bending and effect of forming load. T Nonferr Metal Soc 21(10): 2276-2284
8. Garcia-Romeu ML, Ciurana J, Ferrer I (2007) Springback determination of sheet metals in an air bending process based on an experimental work. J Mater Process Tech 191(1): 174-177
9. Yan Y, Wang HB, Li Q (2015) The inverse parameter identification of Hill 48 yield criterion and its verification in press bending and roll forming process simulations. J Manuf Process 20: 46-53
10. Kim S, Stelson KA (1988) Finite Element Method for the Analysis of a Material Property Identification Algorithm for Pressbrake Bending. J Manuf Sci E 110(3): 218-222
11. Esat V, Darendeliler H, Gokler MI (2002) Finite element analysis of springback in bending of aluminium sheets. Mater Design 23(2): 223-229
12. Zhang DJ, Cui ZS, Ruan XY, Li YQ (2007) An analytical model for predicting springback and side wall curl of sheet after U-bending. Comp Mater Sci 38(4): 707-715
13. Anokye-Siribor K, Singh UP (2000) A new analytical model for pressbrake forming using in-process identification of material characteristics. J Mater Process Tech 99(1): 103-112
14. Zhao J, Yin J, Ma R, Ma LX (2011) Springback equation of small curvature plane bending. Sci China Technol Sc 54(9): 2386-2396
15. Mohammadi S V, Parsa MH, Aghchai AJ (2014) Simplified springback prediction in Al/PP/Al sandwich air bending. J Sandw Struct Mater 17(3): 217-237
16. Huang K, Yang WY (2016) Analytical modeling of residual stress formation in workpiece material due to cutting. Int J Mech Sci 114: 21-34
17. Ma Y, Feng PF, Zhang JF, Wu ZJ, Yu DW (2016) Prediction of surface residual stress after end milling based on cutting force and temperature. J Mater Process Tech 235:41-48
18. Yang D, Liu ZQ, Ren XP, Zhuang P (2016) Hybrid modeling with finite element and statistical methods for residual stress prediction in peripheral milling of titanium alloy Ti-6Al-4V. Int J Mech Sci 108-109: 29-38
19. Agrawal S, Joshi SS (2013) Analytical modelling of residual stresses in orthogonal machining of AISI4340 steel. J Manuf Process 15(1): 167-179

20. Weiss M, Rolfe B, Hodgson PD, Yang CH (2012) Effect of residual stress on the bending of aluminium. J Mater Process Tech 212(4): 877-883
21. Abvabi A, Rolfe B, Hodgson PD, Weiss M (2016) An inverse routine to predict residual stress in sheet material. Materials Science and Engineering: A 652: 99-104
22. Abvabi A, Rolfe B, Hodgson PD, Weiss M (2015) The influence of residual stress on a roll forming process. Int J Mech Sci 101-102:124-136
23. Lin C, Peng Y, Sun JL (2013) Theoretical analysis on springback in bending considering the initial residual stress. Engineering Mechanics 30(9): 28-33
24. Singh A, Agrawal A (2015) Investigation of surface residual stress distribution in deformation machining process for aluminum alloy. J Mater Process Tech 225: 195-202
25. Huang XM, Sun J, Li JF (2015) Finite element simulation and experimental investigation on the residual stress-related monolithic component deformation. Int J Adv Manuf Tech 77(5-8): 1035-1041
26. Wang M, Liu YN, Sun GZ (2017) Influence of Initial Residual Stress and Cutting Stress on Machining Deformation of Thin-walled Parts. Journal of Beijing University of Technology 43(8): 1141-1147
27. Spence TW, Makhlouf MM (2015) The effect of machining-induced residual stresses on the creep characteristics of aluminum alloys. Materials Science and Engineering: A 630(4): 125-130
28. Lam ACL, Shi ZS, Lin JG, Huang X (2015) Influences of residual stresses and initial distortion on springback prediction of 7B04-T651 aluminium plates in creep-age forming. Int J Mech Sci 103:115-126
29. Li WD, Ma LX, Wan M, Peng JW, Meng B (2018) Modeling and simulation of machining distortion of pre-bent aluminum alloy plate. J Mater Process Tech 258: 189-199
30. Quach WM, Teng JG, Chung KF (2006) Finite element predictions of residual stresses in press-braked thin-walled steel sections. Eng Struct 28(11): 1609-1619
31. Quach WM, Teng JG, chung KF (2010) Effect of the manufacturing process on the behaviour of press-braked thin-walled steel columns. Eng Struct 32(11): 3501-3515
32. Li Y, Shi ZS, Lin JG, Yang YL, Saillard P, Said R (2018) Effect of machining-induced residual stress on springback of creep age formed AA2050 plates with asymmetric creep-ageing behavior. Int J Mach Tool Manu 132:113-122
33. Li JG, Wang SQ (2017) Distortion caused by residual stresses in machining aeronautical aluminum alloy parts: recent advances. Int J Adv Manuf Tech 89(1-4): 997-1012
34. Huang XM, Sun J, Li JF, Han X, Xiong QC (2013) An Experimental Investigation of Residual Stresses in High-Speed End Milling 7050-T7451 Aluminum Alloy. Adv Mech Eng 2013(2): 435-447
35. Mohammadpour M, Razfar MR, Saffar RJ (2010) Numerical investigating the effect of machining parameters on residual stresses in orthogonal cutting. Simul Model Pract Th 18(3): 378-389
36. Tang ZT, Liu ZQ, Ai X (2008) Experimentation on the Superficial Residual Stresses Generated by High-speed Milling Aluminum Alloy. China Mechanical Engineering 19: 699-703

37. Kim H, Nargundkar N, Altan T (2007) Prediction of Bend Allowance and Springback in Air Bending. J Manuf Sci E 129(2): 342-351
38. Henrard C, Bouffioux C, Eyckens P et al (2011) Forming forces in single point incremental forming: prediction by finite element simulations, validation and sensitivity. Comput Mech 47(5): 573-590
39. Chatti S, Hermi N (2011) The effect of non-linear recovery on springback prediction. Comput Struct 89(13-14): 1367-1377
40. Zhang ZT, Hu S J (1998) Stress and residual stress distributions in plane strain bending. Int J Mech Sci 40(6): 533-543
41. Zhang M and Tian XT (2020) Residual stresses and strains analysis in press-braking bending parts considering multi-step forming effect. P I Mech Eng B-J Eng 234(4): 788–800
42. Yang X, Choi C, Sever NK et al (2016) Prediction of springback in air-bending of Advanced High Strength steel (DP780) considering Young s modulus variation and with a piecewise hardening function. Int J Mech Sci 105(1-2): 266-272
43. Li H, Yang H, Song FF, Zhan M, Li GJ (2012) Springback characterization and behaviors of high-strength Ti–3Al–2.5V tube in cold rotary draw bending. J Mater Process Tech 212(9):1973-1987
44. Shen W, Yan RJ, Li SY, Xu L (2018) Spring-back analysis in the cold-forming process of ship hull plates. Int J Adv Manuf Tech 96:2341-2354
45. Abvabi A, Rolfe B, Hodgson PD, Weiss M (2014) Effect of temper rolling on final shape defects in a V-section roll forming process. American Institute of Physics Conference Series 1567(1): 896-899
46. Parsa MH, Mohammadi SV, Mohseni E (2015) Thickness change and springback of cold roll bonded aluminum/copper clad sheets in air bending process. P I Mech Eng B-J Eng 231(4): 675-689

Figures

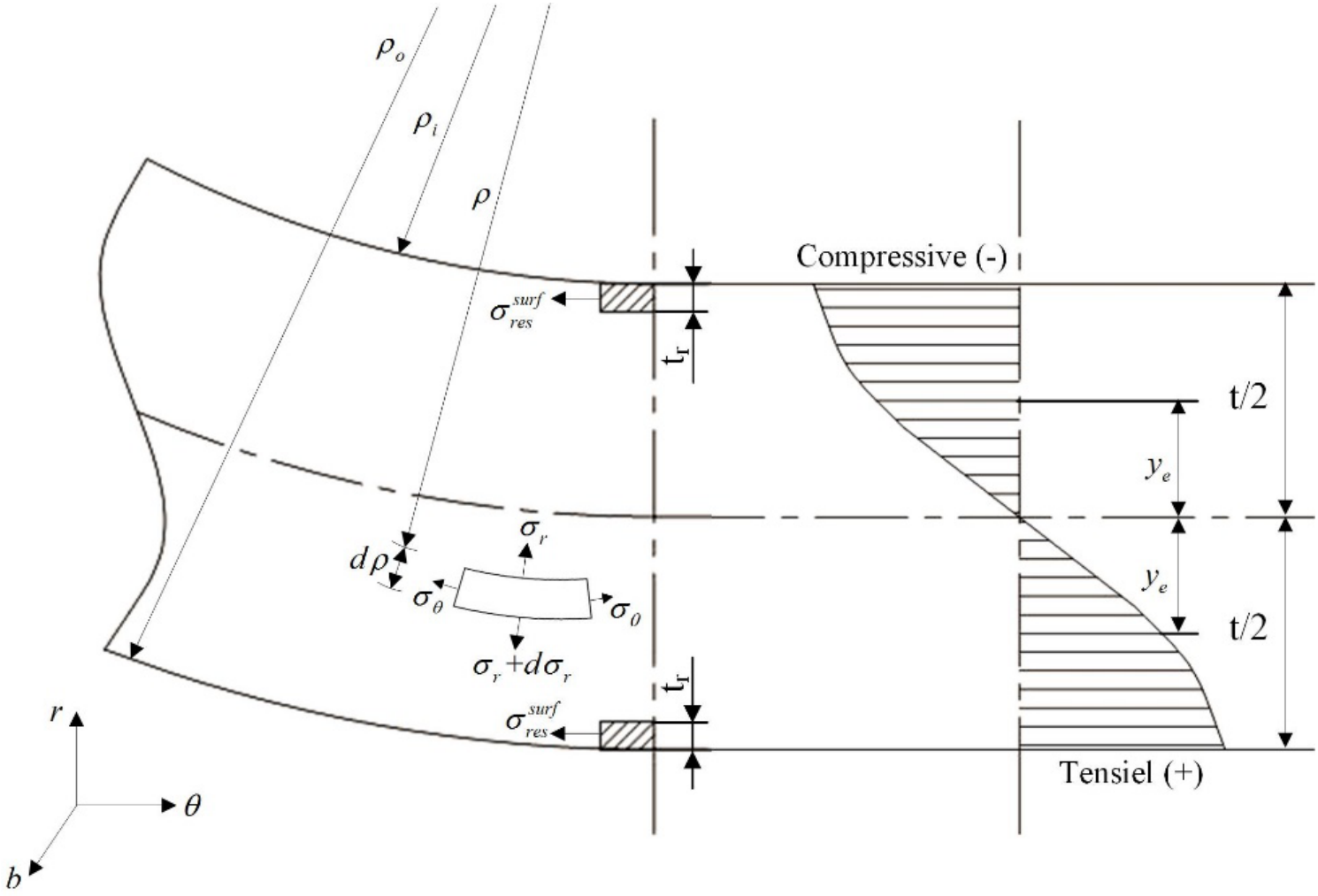

Figure 1

Stress distributions through the material thickness considering the initial stress

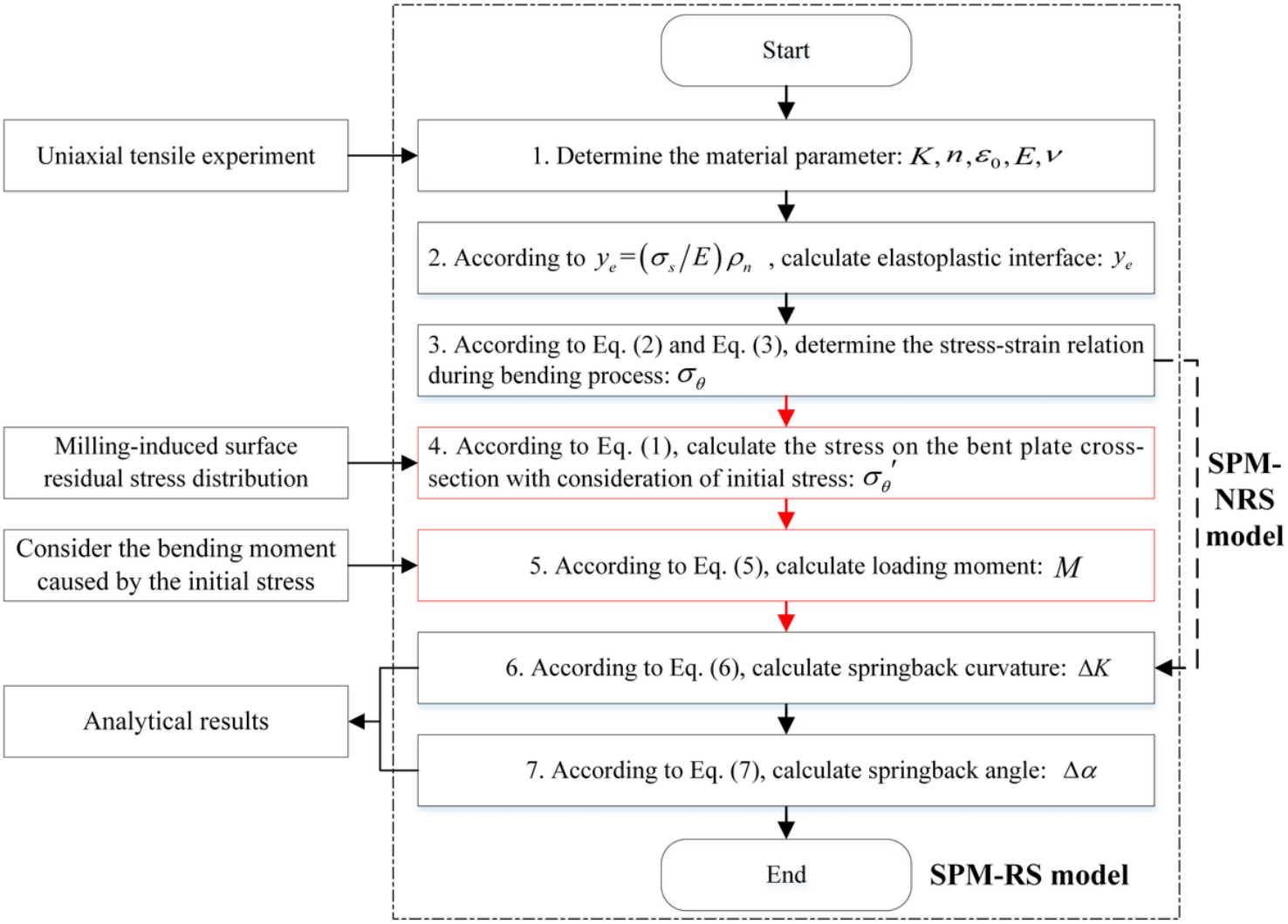

Figure 2

Flowchart used to solve the springback curvature and springback angle

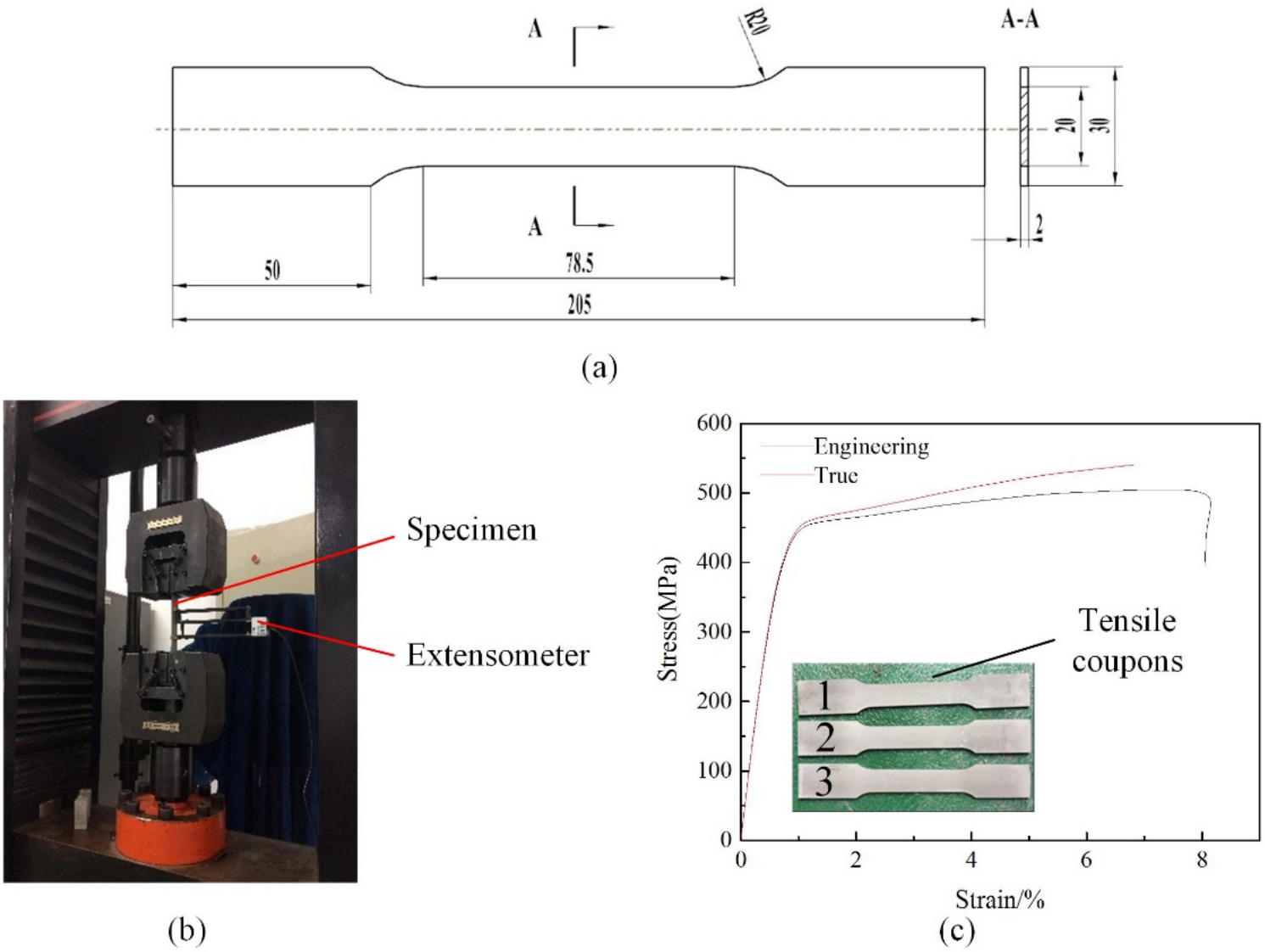

Figure 3

Mechanical properties test (a) tensile specimen (b) tensile process (c) stress-strain curves

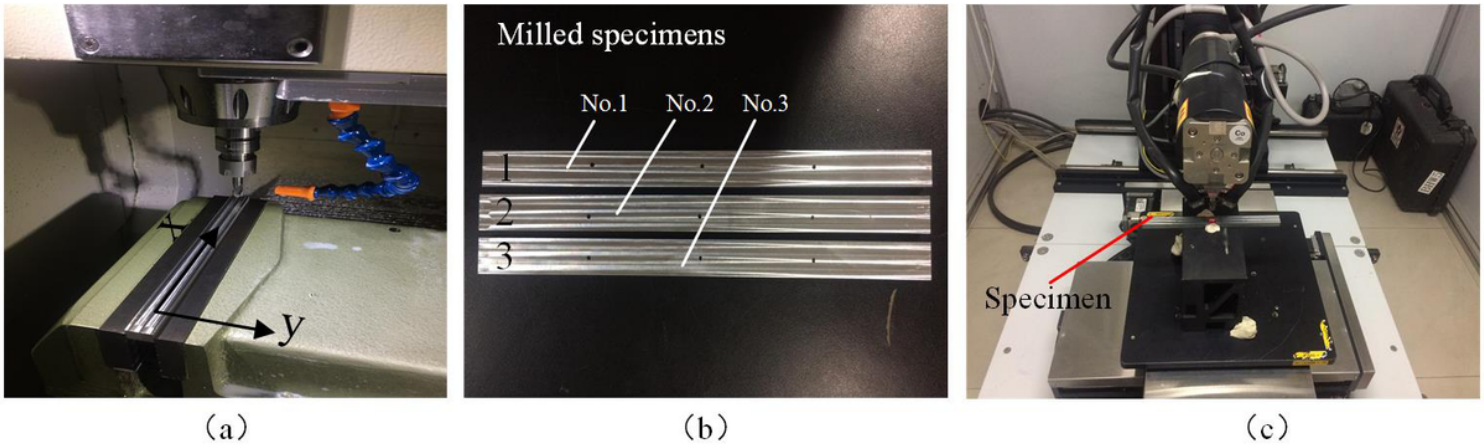

Figure 4

Milling process and measurement of the surface residual stress (a) milling process (b) specimens after milling (c) residual stress measurement

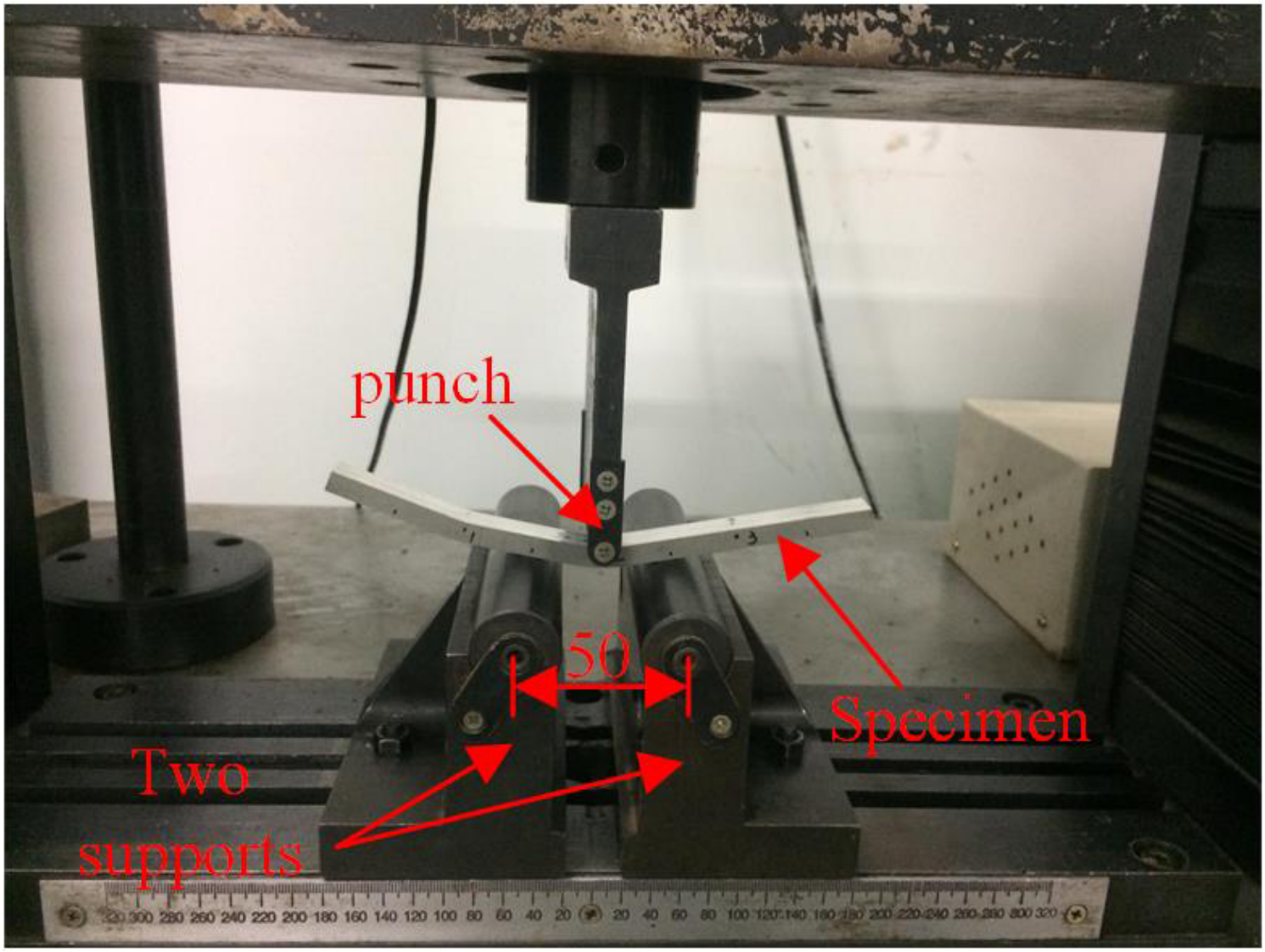

Figure 5

Bending experiment

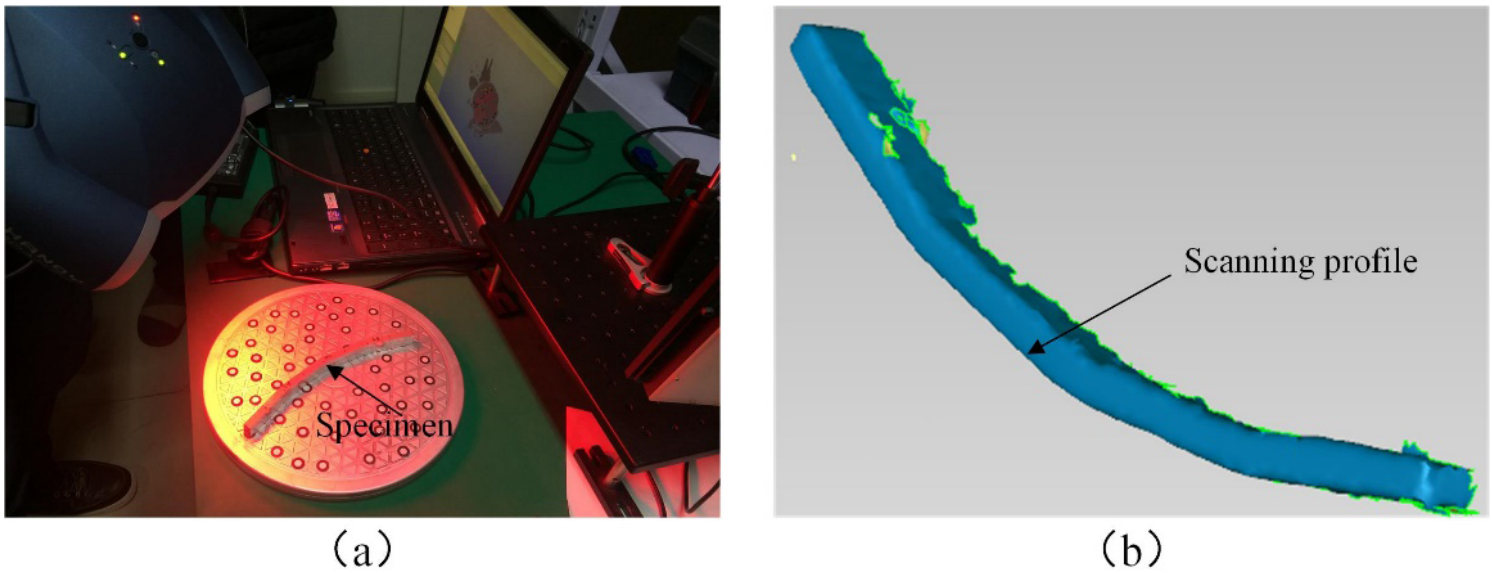

Figure 6

(a) Scan the workpiece profile (b) the contour of the specimen after data processing

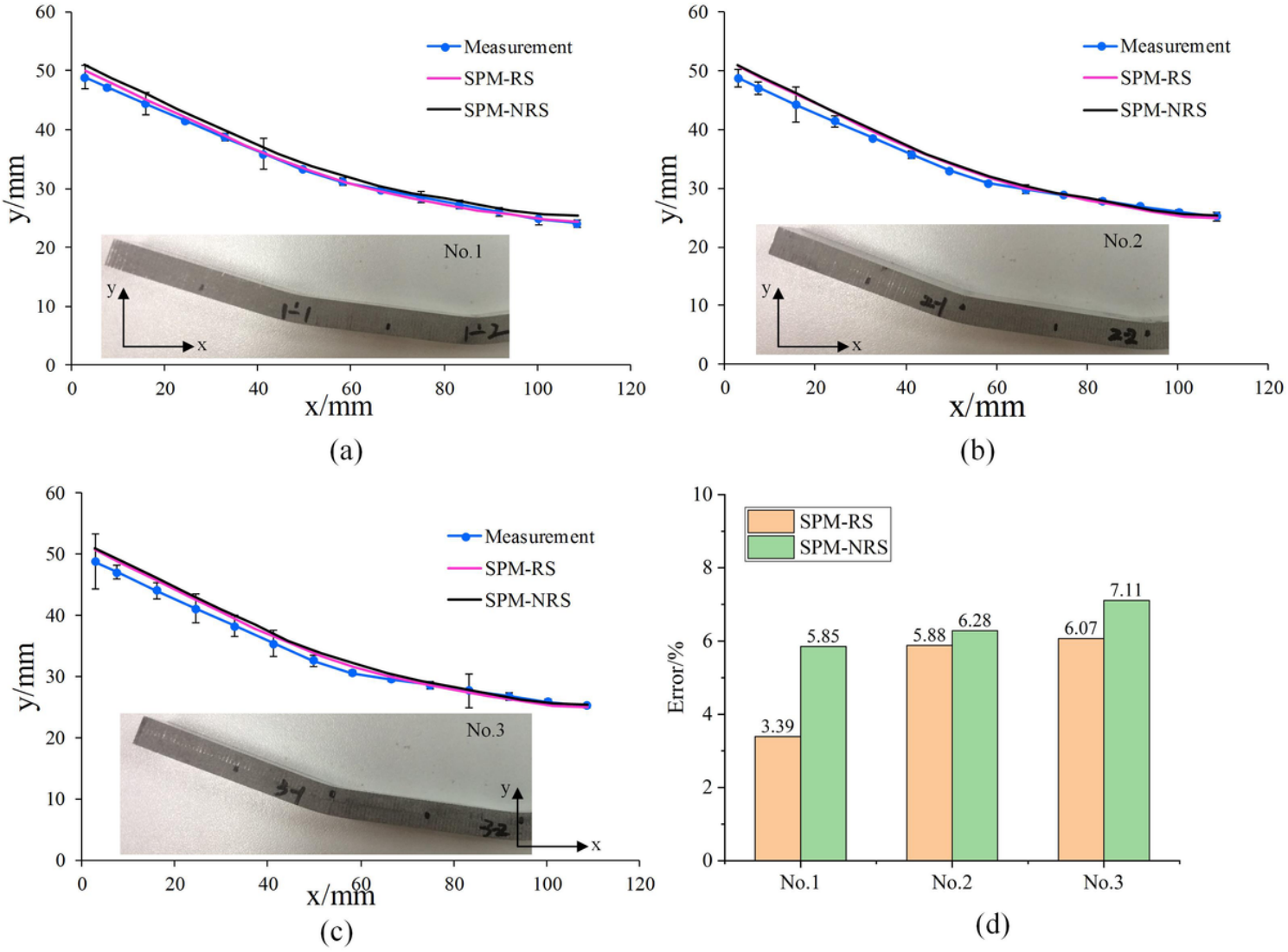

Figure 7

The profile of three test plates after springback determined experimentally and by the analytical approach (a) No.1 (b) No.2 (c) No.3 (d) maximum contour deflection

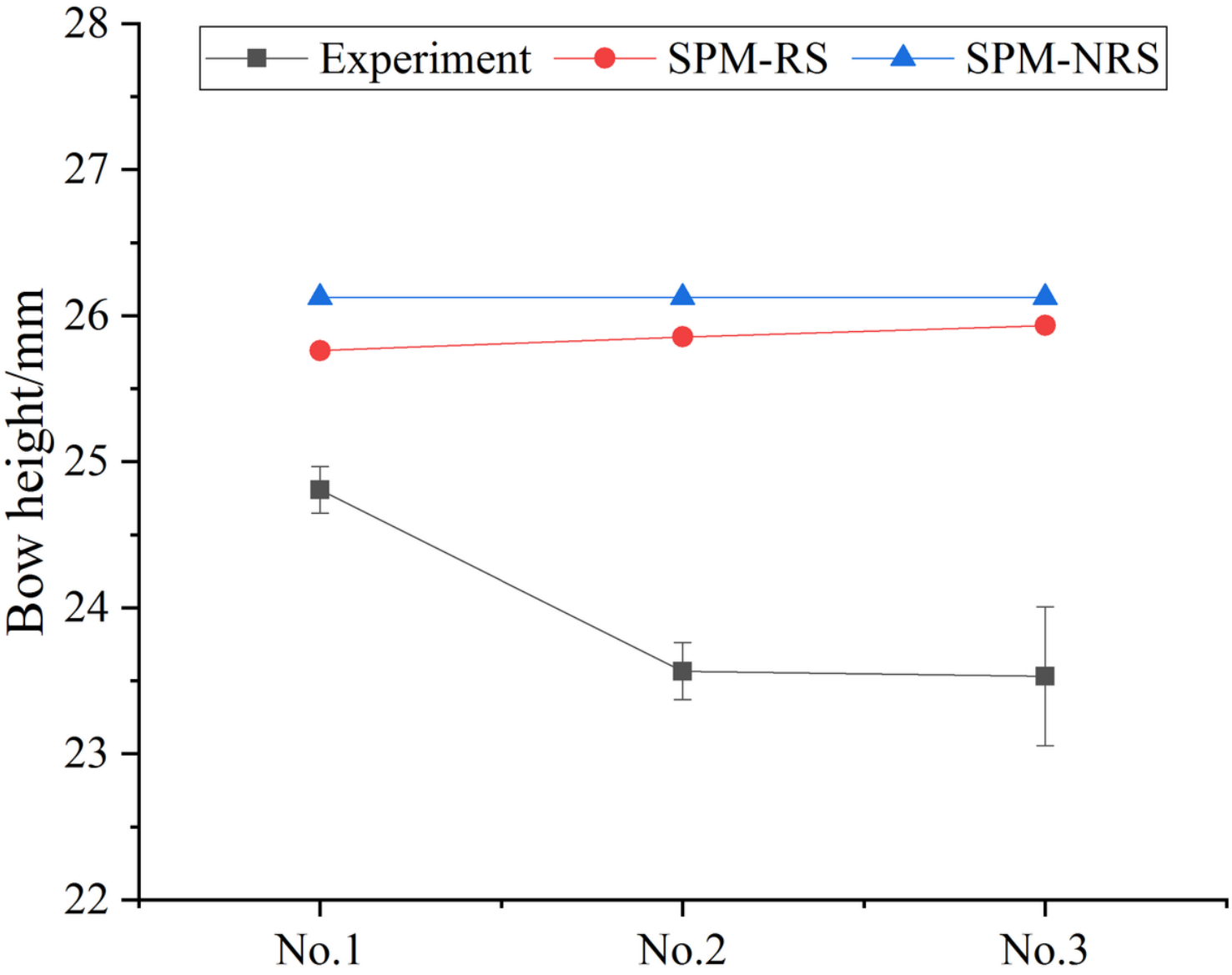

Figure 8

Comparison of bow height

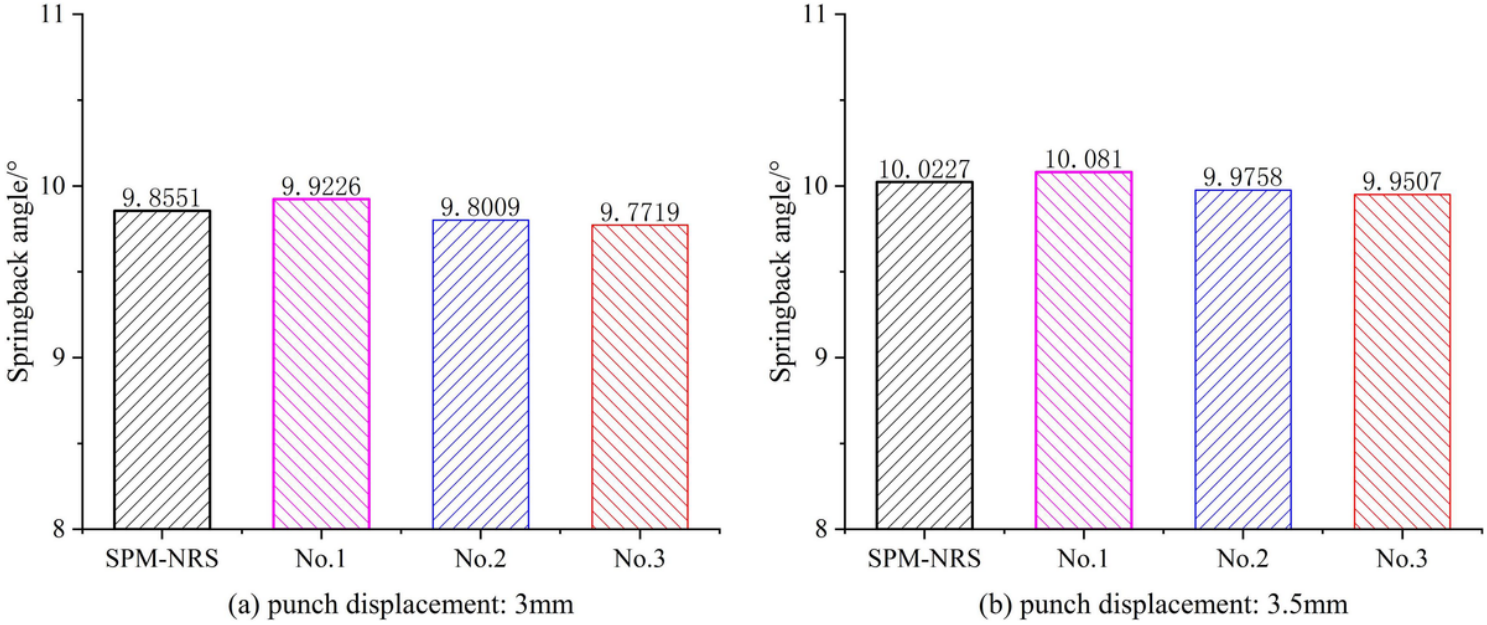

Figure 9

Comparison of springback angle (a) punch displacement: 3mm (b) punch displacement: 3.5mm

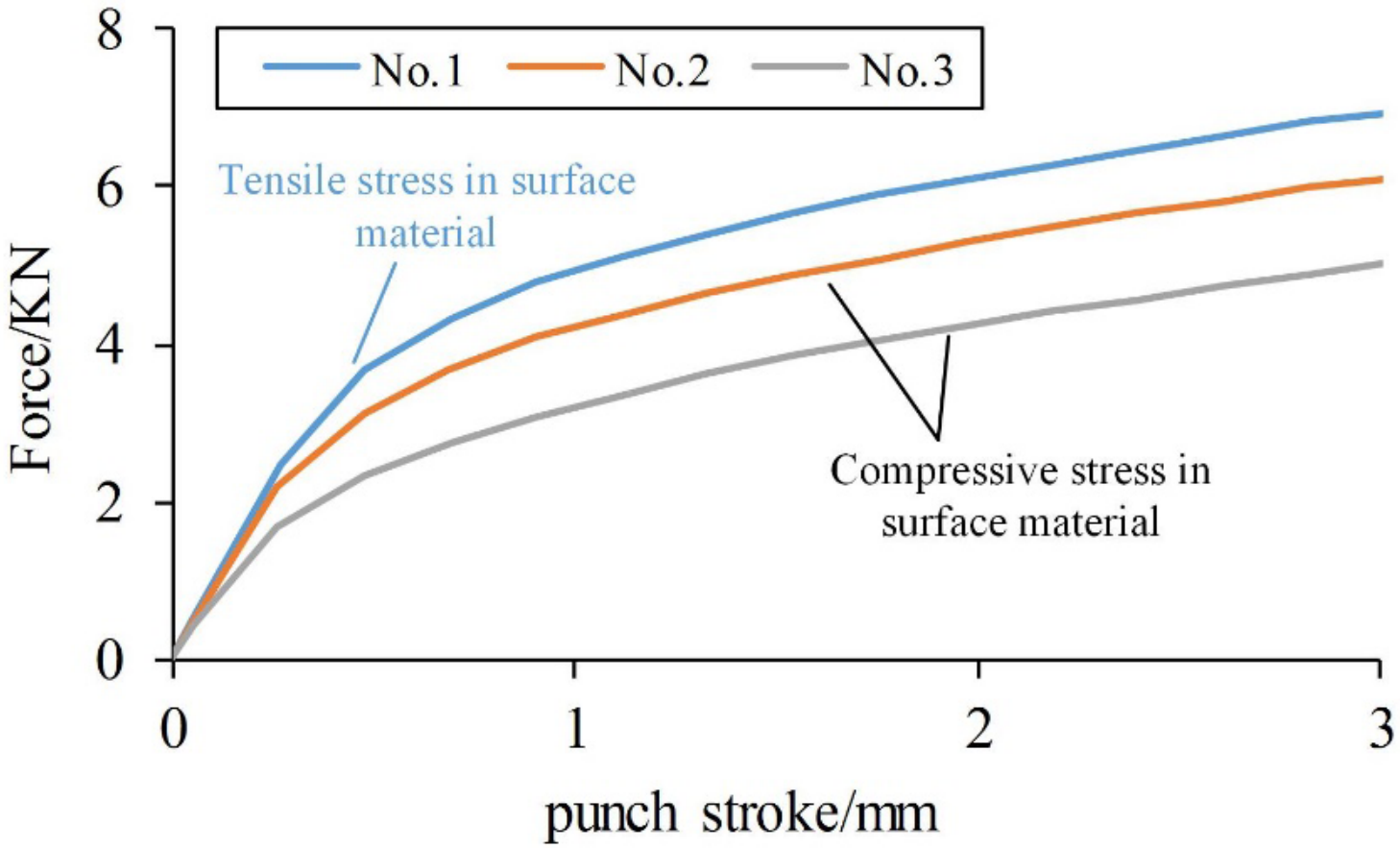

Figure 10

Force-displacement curves under punch stroke of 3mm during loading